cases, from Table I) are candidates for D_{5d} or D_{3d} symmetry, but not T_h.

Acknowledgment. We wish to thank Drs. Harry Brittain, Robert Detrano, and Mr. Joseph Ruggio for their assistance with the programming and Professor William Berkowitz for several helpful discussions. A grant-in-aid from the CUNY research foundation (No. RF 10202) is gratefully acknowledged.

References and Notes

(1) Alfred P. Sloan Research Fellow.
(2) The remaining two regular polyhedra, the octahedron and the icosahedron, are not suitable skeletons for neutral hydrocarbons as they imply pentavalent carbons. We have in fact found that octahedrane distorts into D_{2d} symmetry by a second-order Jahn-Teller mechanism.
(3) P. E. Eaton and T. V. Cole, Jr., *J. Am. Chem. Soc.*, **86**, 3157 (1964).
(4) S. B. Fleischer, *J. Am. Chem. Soc.*, **86**, 3889 (1964).
(5) J. M. Schulman and T. Venanzi, *J. Am. Chem. Soc.*, **96**, 4739 (1974).
(6) For a discussion of bond-angle strain in polyhedranes, see H. P. Schultz, *J. Org. Chem.*, **30**, 1361 (1965).
(7) Aspects of factorization of the secular equation of polyhedral molecules are discussed by R. Hoffmann and W. N. Lipscomb, *J. Chem. Phys.*, **36**, 2179 (1962).
(8) For descriptions of recent work directed toward the synthesis of dodecahedrane, see (a) R. B. Woodward, T. Fukunaga, and R. C. Kelly, *J. Am. Chem. Soc.*, **86**, 3162 (1964); (b) L. A. Paquette, G. V. Meehan, and S. J. Marshall, *ibid.*, **91**, 6779 (1969); (c) P. E. Eaton and R. H. Mueller, *ibid.*, **94**, 1014 (1972); (d) I. T. Jacobsen, *Chem. Scr.*, **5**, 174 (1974).
(9) $B_{12}H_{12}^{2-}$ is also of icosahedral symmetry if its counterions are ignored. Strictly speaking, this group should be named I_i as it is the direct product of the group I with i; there are no reflection planes perpendicular to the fivefold axes.
(10) For the 2^5- and 2^6-pole moments the names *triakontadipole* and *hexakontatessarapole*, respectively, are obtained in the conventional nomenclature. For obvious reasons, we do not advocate their usage.
(11) (a) A. D. Buckingham, "Physical Chemistry, An Advanced Treatise", D. Henderson, Ed., Academic Press, New York, N.Y., 1970, p 349; (b) L. L. Boyle and Z. Ozgo, *Int. J. Quantum Chem.*, 7, 383 (1973).
(12) Contributions to the second virial coefficients of progressively more spherical hard convex polyhedra have been considered by T. Kihara, *J. Chem. Soc. Jpn.*, **6**, 289 (1951), and shown to converge rapidly to the hard sphere limit.
(13) B. D. Kybett, S. Caroll, P. Natalis, D. W. Bonnell, J. L. Margrave, and J. L. Franklin, *J. Am. Chem. Soc.*, **88**, 626 (1966). Another such example is adamantane of T_d symmetry for which $\Delta H_{s332°K} = 14.0$ kcal mol; W. K. Bratton, I. Szilard, and C. A. Cupas, *J. Org. Chem.*, **32**, 2019 (1967).
(14) The dihedral angle between pentagonal faces is 116°34′.
(15) E. M. Engler, J. D. Andose, and P. v. R. Schleyer, *J. Am. Chem. Soc.*, **95**, 8005 (1973).
(16) Alternatively, a planar graph is a graph which can be embedded in a plane, i.e., faithfully represented by points and lines drawn in the plane such that no two lines meet, except at a vertex: J. W. Essam and M. E. Fisher, *Rev. Mod. Phys.*, **42**, 282 (1970).
(17) L. A. Lyusternik, "Convex Figures and Polyhedra", Dover Publications, New York, N.Y., 1963, p 53.
(18) F. Harary, Ed., "A Seminar on Graph Theory", Holt, Rinehart and Winston, New York, N.Y., 1967. It can be shown that a cubic, hamiltonian graph has at least three spanning cycles.
(19) The IUPAC names for tetrahedrane and cubane are tricyclo[1.1.0.$0^{2,4}$]butane and pentacyclo[4.2.0.$0^{2,5}$.$0^{3,8}$.$0^{4,7}$]octane, respectively. These names are based on the extended von Baeyer method (IUPAC rules A-31 and A-32). See also D. R. Eckroth, *J. Org. Chem.*, **32**, 3362 (1967).
(20) (a) J. H. Redfield, *Am. J. Math.*, **49**, 433 (1927); (b) G. Pólya, *Helv. Chim. Acta*, **19**, 22 (1936).
(21) B. A. Kennedy, D. A. McQuarrie, and C. H. Brubaker, Jr., *Inorg. Chem.*, **3**, 265 (1964). For a review of isomer enumeration methods, see D. H. Rouvray, *Chem. Soc. Rev.*, **3**, 355 (1974).
(22) The unoccupied orbitals in this valence basis transform as $a_g(1)$, $t_{1g}(1)$, $t_{2g}(1)$, $h_u(1)$, $t_{1u}(2)$, $t_{2u}(2)$, $g_g(2)$, $g_u(2)$, and $h_g(2)$. It may be shown that the number of linear variational parameters in this valence set SCF calculation is only 25; each symmetry species contributes $n_{occ}n_{unocc}$ variational degrees of freedom where n_{occ} and n_{unocc} are the number of occupied and unoccupied molecular orbitals of that symmetry, respectively.
(23) R. Hoffmann and M. Gouterman, *J. Chem. Phys.*, **36**, 2189 (1962).
(24) G. H. Wannier, *Phys. Rev.*, **64**, 359 (1943).
(25) T. C. Chen, *J. Chem. Phys.*, **29**, 347, 356 (1958).
(26) The ordering of the N_{20} occupied orbitals is $1a_g < 1t_{1u} < 1h_g < 1g_u < 1t_{2u} < 2a_g < 1g_g < 2t_{1u} < 2h_g < 1h_u < 3h_g < 2t_{2u} < 2g_u < 2g_g$.
(27) J. W. McIver, Jr., P. Coppens, and D. Nowak, *Chem. Phys. Lett.*, **11**, 82 (1971).

Decomposition Rates of Excited Reaction Complexes. Temperature and Pressure Effects in Association Reactions Involving NH_4^+, $CH_3NH_3^+$, and $(CH_3)_2NH_2^+$

Michael Meot-Ner and F. H. Field*

Contribution from the Chemistry Department, Rockefeller University, New York, New York 10021. *Received February 10, 1975*

Abstract: Kinetic studies were made on clustering reactions involving NH_4^+, $CH_3NH_3^+$, and $(CH_3)_2NH_2^+$ between 250 and 400°K. The association reactions $BH^+ + B + M \rightarrow B_2H^+ + M$ (B = CH_3NH_2, $(CH_3)_2NH$) exhibit transitions between second- and third-order kinetics in the pressure range 0.5–2.0 Torr and the temperature range 250–400°K. The dependence of the overall forward rate constants on third-body pressure confirms the energy transfer mechanism $BH^+ + B \rightleftharpoons B_2H^+*$ followed by $B_2H^+* + M \rightarrow B_2H^+ + M$. The dissociation rate constants, k_b, of the excited complexes and their temperature dependences are [given respectively as excited complex, k_b^{350} (10^7 sec^{-1}), T dependence of k_b]: $(NH_4^+ \cdot NH_3)^*$, 220, $T^{3.2}$; $(CH_3NH_3^+ \cdot CH_3NH_2)^*$, 12, $T^{3.6}$; $((CH_3)_2NH_2^+ \cdot (CH_3)_2NH)^*$, 6.0, $T^{7.2}$. The decrease of the rate constants with increasing molecular complexity and the increase with increasing temperature are quantitatively accounted for by calculations based on an RRKM coupled quantum oscillator model.

The kinetics of the decomposition processes of excited reaction intermediates is a problem of central significance in determining the rates and results of chemical reactions. The study of reactions with well-established mechanisms can provide relatively straightforward information on decomposition rates and lifetimes of excited reaction complexes and the effects of the structure, complexity, and energy content on the decomposition rates of such species. The present paper reports the results of studies on the mechanism of clustering reactions of the ions NH_4^+, $CH_3NH_3^+$, and $(CH_3)_2NH_2^+$ and the effects of temperature and molecular complexity on the decomposition rates of the excited ion-molecule association complexes $(NH_4^+ \cdot NH_3)^*$, $(CH_3NH_3^+ \cdot CH_3NH_2)^*$, and $((CH_3)_2NH_2^+ \cdot$

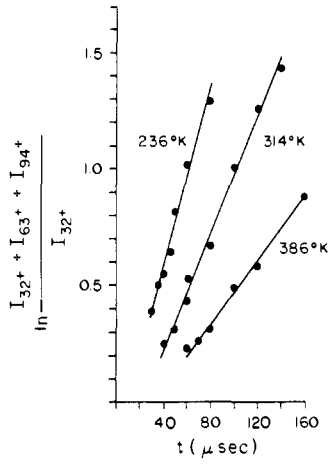

Figure 1. Sample pseudo-first-order kinetic plots for the association reaction $CH_3NH_3^+$ (*m/e* 32) + CH_3NH_2 + *i*-C_4H_{10} → $(CH_3NH_2)_2H^+$ (*m/e* 63) + *i*-C_4H_{10}. Experimental conditions: $(M)_{i\text{-}C_4H_{10}} \approx 1.9 \times 10^{16}$ mol/cm.^{3}; $P_{CH_3NH_2}/P_{i\text{-}C_4H_{10}} = 0.00229$. The higher mass ion $(CH_3NH_2)_2H^+$, *m/e* 94, when present, is assumed to be formed by a consecutive reaction of $(CH_3NH_2)_2H^+$. Note that since the association reactions are preceded by the protonation of CH_3NH_2 by *t*-$C_4H_9^+$ to form $CH_3NH_3^+$, the kinetic plots intercept the ordinate at $t \approx 30$ μsec rather than at $t = 0$.

$(CH_3)_2NH)^*$. Some experiments were also done on clustering reactions of the larger alkylamine ions $C_2H_5(CH_3)_2NH^+$ and $(C_3H_7)_2NH_2^+$.

Experimental Section

The present studies were conducted on The Rockefeller University Chemical Physics mass spectrometer.[1] The experimental technique of pulsed, high-pressure mass spectrometry was applied. In this method ions are generated by the bombardment of the reaction mixture by a 5–10 μsec long pulse of 600 V electrons. The reactions take place in conditions free of repeller and magnetic fields and the relative concentrations of the ions leaving the source are measured explicitly as a function of reaction time. The reactions were studied in mixtures of ≈1% NH_3 in CH_4 and ≈1% CH_3NH_2 or $(CH_3)_2NH$ in *i*-C_4H_{10}. Total pressures of 0.5–2.0 Torr were used. Under these conditions most of the major ions of the reactant gas (CH_5^+ and $C_2H_5^+$; *t*-$C_4H_9^+$) react by fast H^+ transfer reactions to produce the protonated ions NH_4^+, $CH_3NH_3^+$, and $(CH_3)_2NH_2^+$. The protonated ions then react more slowly with additional molecules of the additive amine to form the association products $(NH_3)_2H^+$, $(CH_3NH_2)_2H^+$, and $((CH_3)_2NH)_2H^+$. In most cases the reaction systems were sufficiently removed from equilibrium that opposing dissociation reactions of the reaction products could be neglected; however, in some measurements at higher temperatures the opposing reactions were also considered. The kinetic analysis applied to the results was also described in previous publications.[2,3] Sample kinetic plots are shown in Figure 1.

The overall forward reaction may be written as

$$BH^+ + B \xrightarrow{M} B_2H^+ \quad (1)$$

Since the concentration of the ions in the reaction mixtures is much smaller than the concentration of the neutrals, the kinetic measurements yield pseudo-first-order rate constants, k_1, for the disappearance of BH^+. From these the second-order rate constants are obtained as

$$k_f = k_1/(B) \quad (2)$$

The reproducibility of the rate constant measurements in each of the systems studied was found to be better than ±10%.

We performed several measurements to check the agreement of the results of our measurements using the pulsed high-pressure mass spectrometric technique with published or theoretically expected equilibrium and rate constants. Using the pulsed technique to establish the attainment of equilibrium,[2,3] we measured the equilibrium constant for the reaction $(CH_3)_2NH_2^+ + (CH_3)_2NH_4$ + *i*-C_4H_{10} ⇌ $((CH_3)_2NH)_2H^+$ + *i*-C_4H_{10} at 431, 437, and 468°K and obtained from the resultant van't Hoff plot for this reaction the values: $\Delta H = -22.0$ kcal/mol, $\Delta S = -25.3$ eu. These are in good agreement with the values published by Yamdagni and Kebarle:[4] $\Delta H = -20.8$ kcal/mol, $\Delta S = -25.7$ eu. Similarly, we obtained for the reaction $C_2H_5(CH_3)_2NH^+ + C_2H_5(CH_3)_2N$ + *i*-C_4H_{10} ⇌ $(C_2H_5(CH_3)_2N)_2H^+$ + *i*-C_4H_{10}, $\Delta H = -20.2$ kcal/mol, $\Delta S = -29.6$ eu, in good agreement with published values for the analogous reaction involving the similar compound $(CH_3)_3N$, $\Delta H = -22.5$ kcal/mol, $\Delta S = -32$ eu.[4] As a check on rate constant measurements, we obtained for the reaction *t*-$C_4H_9^+$ + $(CH_3)_2NH$ → $(CH_3)_2NH_2^+ + C_4H_8$ (k) the value $k_{400°K} = 1.45 \times 10^{-9}$ cm^3/(mol sec), and for the H^+ transfer reaction from *t*-$C_4H_9^+$ to $(C_3H_7)_2NH$, $k_{400°K} = 1.53 \times 10^{-9}$ cm^3/(mol sec). These results are in good agreement with the rate constants predicted for these reactions by the parameterized average dipole orientation theory,[5] 1.34×10^{-9} and 1.48×10^{-9} cm^3/(mol sec), respectively; the former is also in good agreement with a measured experimental value,[6] 1.2×10^{-9} cm^3/(mol sec).

As a further check on our technique we tested for the possibility of significant collisional dissociation of the B_2H^+ ions in the region outside the source between the ion exit slit and ion focus plates. For this purpose we varied the potential difference between the ion exit slit and the ion focus plates, thereby varying the field strength in this region between 40 and 360 V/cm. We observed no effect of the field strength on the ion intensity ratio $I_{B_2H^+}/I_{BH^+}$. This indicates that collisional dissociation of the cluster ions is unlikely to be significant.

In summary, we observe that the results of our measurements using the pulsed ionization technique are in very good agreement with published results obtained with an instrument with a somewhat different source geometry,[4] and with theoretically expected results. Based on these reactions, we believe that our measured rate constants are accurate within 10% in absolute magnitude.

Results

1. Reaction Mechanism. Pressure Studies. The mechanism of three-body ion-molecule association reactions is generally assumed to be the energy transfer mechanism:[7]

$$BH^+ + B \underset{k_b}{\overset{k_c}{\rightleftharpoons}} B_2H^{+*} \quad (3)$$

$$B_2H^{+*} + M \xrightarrow{k_s} B_2H^+ + M \quad (4)$$

The overall forward rate constant k_f may be defined by

$$\frac{d(B_2H^+)}{dt} = -\frac{d(BH)^+}{dt} = k_f(BH^+)(B) \quad (5)$$

If steady state considerations are applied to the concentration of the excited reaction complex B_2H^{+*}, it is readily shown that the overall forward reaction rate constant for the formation of the product ion B_2H^+ is given by

$$k_f = k_c k_s(M)/[k_b + k_s(M)] \quad (6)$$

If the rate of back-dissociation of the excited complex B_2H^{+*} is significantly larger than the rate of its deactivation, i.e., $k_b \gg k_s(M)$, then $k_f \approx k_c k_s(M)/k_b$, and the reaction exhibits third-order behavior. Most ion-molecule association reactions reported so far exhibit third-order behavior. On the other hand, if $k_s(M) \gg k_b$, $k_f = k_c$ and the association reaction proceeds with unit collision efficiency and exhibits second-order kinetics. In intermediate cases eq 6 may be used to predict the dependence of k_f on (M). Comparison with experiment may then be used to test the applicability of the energy-transfer mechanism to the reactions of interest.

It is of interest to demonstrate the applicability of the energy-transfer mechanism to ion-molecule association reactions, since, although generally assumed, this does not appear to have been done before. A transition from third- to second-order kinetics in the clustering reactions of O_2^+ and N_2^+ with increasing third-order (He) pressure at 80°K was

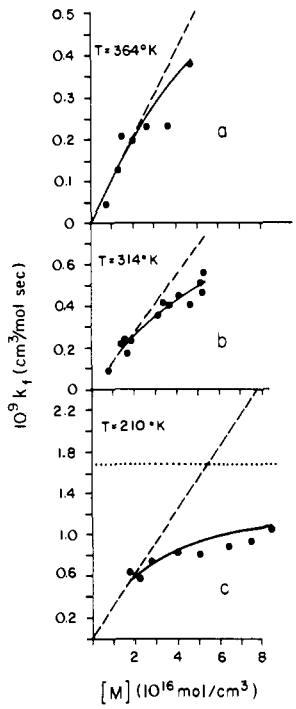

Figure 2. The dependence of the second-order rate constants k_f on third-body density (M) for the reaction $CH_3NH_3^+ + CH_3NH_2$ (M) → $(CH_3NH_3)_2H^+$ at 364, 314, and 210°K. The solid circles (●) are experimental values. The solid lines (—) show the dependence of k_f on (M) as predicted by eq 6 in the text, with the experimental point at (M) = 2×10^{16} mol/cm³ as reference. The broken lines (- - -) show the calculated third-order behavior of k_f based on this reference point. The dotted line in (c) represents the collisional (ADO) second-order capture limit for k_f. M = i-C_4H_{10} in (a) and (b); M = CH_4 in (c). (CH_3NH_2) ≈ 0.01(M) in these experiments.

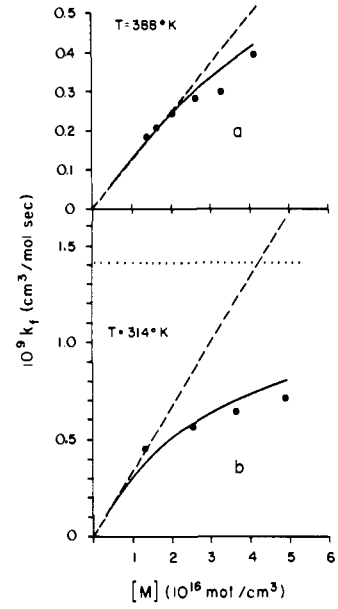

Figure 3. The dependence of the second-order rate constant k_f on third-body (i-C_4H_{10}) density for the reaction $(CH_3)_2NH_2^+ + (CH_3)_2NH$ (M) → $((CH_3)_2NH)_2H^+$. The meaning of the symbols is as in Figure 2. The experimental point at (M) = 1.2×10^{16} mol/cm³ was used as reference for the broken line in Figure 3b.

reported, but the reported transition is much sharper than that predicted by eq 6.[8]

The model for unimolecular decomposition based on the redistribution of energy in a system of coupled oscillators (RRK model) indicates that the lifetime of excited complexes should increase with molecular complexity. Therefore, molecules with a larger number of internal degrees of freedom are good candidates even at moderately high temperatures to permit the magnitude of k_s(M) to approach that of k_b, which is requisite for significant deviation from third-order behavior. Once the mechanism is established, eq 6 may be used in conjunction with measured values of k_f and calculable values of k_c and k_s to obtain k_b, the rate constant for the decomposition of B_2H^+ *, which is of much physical interest.

In Figure 2 we show the experimental dependence of k_f on (M) at 210, 314, and 364°K for reaction II. (Throughout the paper reactions will be referred to according to their number in Table I.) Calculated values of k_f as a function of (M) may be obtained by inverting eq 6, assuming k_c to be equal to the ion-molecule capture collision rate, and evaluating the ratio k_b/k_s from one experimental value of k_f and (M). These calculated values of k_f are represented in Figure 2 by the solid lines, and the agreement with the experimentally observed values is very good. The capture collision rate assumed for k_c is that predicted by the average dipole orientation (ADO) theory, and justification for its use is presented in the next section. At the lowest temperature studied (210°K) the trend of k_f with pressure given in Figure 2 shows that the reaction is predominantly second order in this pressure range. This undoubtedly is the result of a relatively low rate of back-dissociation of the intermediate complex. At higher temperatures the energy of the complex is higher; its dissociation rate is faster; and the pressure dependence of k_f shows that the reaction takes on more third-order character in the pressure range studied. As we show in Figure 3, in the more complex compound $(CH_3)_2NH$ the reaction is closer to second than to third order even at 314°K, and the experimental results agree reasonably well with the predictions of eq 6.

For practical reasons no measurements were made of the effect of pressure on the association reaction in NH_3. Studies were made of the effect of temperature on the NH_3 reaction (see below), and in the course of these we found that NH_3 contaminated the mass spectrometer producing an unacceptable background for a long period of time. Consequently, the applicability of the energy transfer reaction to the ammonia system was assumed throughout the remainder of the work.

2. Decomposition Rates of Excited Reaction Complexes. The Effects of Molecular Complexity. Since the pressure studies on the kinetics of the clustering reactions of $CH_3NH_3^+$ and $(CH_3)_2NH_2^+$ confirm the applicability of the mechanism of eq 3 and 4, we can use eq 6 to calculate the decomposition rates of the excited reaction complexes involved in these reactions.

It is well known that ion-molecule collisions within the critical parameter result in an orbiting ion-molecule complex which brings the reactants into close proximity. Therefore, each collision between BH^+ and B may be considered to result in an excited complex B_2H^+ *, and we can take $k_c = k_{ADO}$. The ADO theory has been shown to account with good accuracy for the rate constants of ion-polar molecule reactions.[5,9,10] For the deactivation processes we selected CH_4 as the third body for the deactivation of $(NH_4^+ \cdot NH_3)$* and i-C_4H_{10} for the deactivation of $(CH_3NH_3^+ \cdot CH_3NH_2)$* and of $((CH_3)_2NH_2^+ \cdot (CH_3)_2NH)$*. The number of internal degrees of freedom in the third bodies in each case is at least one-half of those in the activated complexes. If equilibration of the internal energy takes place in each collision between B_2H^+ * and M, one predicts that at least one-third of the internal excitation energy of B_2H* is removed in each collision. Since the internal excitation energy may be taken equal to the dissociation energy of B_2H^+

Table I. Experimental Rate Constants for Clustering Reactions of NH_4^+, $CH_3NH_3^+$, and $(CH_3)_2NH_2^+$

Designation	Reaction	M	[M] × 10^{-16}, mol/cm³	$k_c \times 10^9$,[a] cm³/(mol sec) 250°K	$k_c \times 10^9$,[a] cm³/(mol sec) 350°K	$k_s \times 10^9$,[b] cm³ (mol sec)	$k_f \times 10^9$,[c] cm³/(mol sec) 250°K	$k_f \times 10^9$,[c] cm³/(mol sec) 350°K	Calcd 3rd-order rate[d] constants $k_3 = k_c k_s / k_b$, 10^{-27} cm⁶/(mol² sec) 250°K	Calcd 3rd-order rate[d] constants $k_3 = k_c k_s / k_b$, 10^{-27} cm⁶/(mol² sec) 350°K
I	$NH_4^+ + NH_3 \xrightarrow{k_f} (NH_3)_2H^+$	CH_4	2.5	2.4	2.1	1.3	0.093	0.030	3.9	1.3[e]
II	$CH_3NH_3^+ + CH_3NH_2 \xrightarrow{k_f} (CH_3NH_2)_2H^+$	i-C_4H_{10}	1.8	1.7	1.6	1.2	0.40	0.23	30	16
III	$(CH_3)_2NH_2^+ + (CH_3)_2NH \xrightarrow{k_f} ((CH_3)_2NH)_2H^+$	i-C_4H_{10}	1.6		1.4	1.1		0.32		26

[a] Capture collision rate constant for the process $BH^+ + B \rightarrow B_2H^{+*}$. Since the neutral species are polar molecules, the parametrized ADO theory was used to calculate the rate constants. [b] Capture collision rate constants for the process $B_2H^{+*} + M \rightarrow B_2H^+ + M$. Since CH_4 is nonpolar and the dipole moment of i-C_4H_{10} is small, the ADO and Langevin equations give similar rate constants for these processes. These rate constants are not temperature dependent. [c] k_f is calculated from the pseudo-first-order rate constants k_1 which are directly measured in these experiments, i.e., $k_f = k_1/(B)$ where (B) is the number density of the neutral reactant B (mol/cm³). [d] k_3 is the third-order rate constant for the association reaction. Since our reactions deviate from third order, k_3 is not generally directly available from our experimental observations. It is available as an approximation only under low-pressure conditions. It is presented here to facilitate comparison with rate constants for other ion–molecule association reactions, which are usually published as third-order rate constants. [e] D. K. Bohme and F. C. Fehsenfeld, *Can. J. Chem.*, 47, 2715 (1969), reported for the reaction: $NH_4^+ + NH_3 + O_2 \rightarrow (NH_3)_2H^+ + O_2$, $k_3^{298} = 1.8 \times 10^{-27}$ cm⁶/(mol² sec). Considering the higher third-body efficiency of CH_4, this compares well with the rate calculated from our data at 298°K: $k_3^{298} = 2.4 \times 10^{-27}$ cm⁶/(mol² sec).

Table II. Dissociative Half-Lives, Decomposition Rate Constants, and Temperature Dependence for Excited Reaction Complexes B_2H^{+*}

Complex	k_b (exptl),[a] 10^7 sec⁻¹ 250°K	k_b (exptl),[a] 10^7 sec⁻¹ 350°K	Dissociative half-life of B_2H^{+*} (τ_b), 10^{-9} sec 250°K	Dissociative half-life of B_2H^{+*} (τ_b), 10^{-9} sec 350°K	Temp dependence of k_b[b]
$(NH_4^+ \cdot NH_3)^*$	81	220	0.86	0.32	$T^{3.2}$
$(CH_3NH_3^+ \cdot CH_3NH_2)^*$	6.8	12	10	5.8	$T^{3.6}$
$((CH_3)_2NH_2^+ \cdot (CH_3)_2NH)^*$		6.0		12	$T^{7.2}$

[a] Obtained from k_f of the corresponding association reaction, the values of k_c and k_s as given in Table I, and eq 6 in text. [b] From the slopes of the plots of ln k_b vs. ln T at 375°K in Figure 4.

(≈20 kcal/mol), the removal of 6–7 kcal/mol from B_2H^{+*} will make the back dissociation of this complex negligibly slow. Therefore, the use of these efficient third bodies makes the assumption $k_s \approx k_{Langevin}$ or k_{ADO} reasonable, and we used these values (Table I), the measured values of k_f, and eq 6 to calculate k_b, the dissociation rate constants for the activated complexes over a range of temperatures. The values of the quantities used in the calculations are given in Table I.

The values of k_b for the reactions of this study obtained in the above manner at 250 and 350° are shown in Table II. The absolute values of the dissociation rates of the excited complexes show the dependence on molecular complexity as may be expected; namely, the rate decreases as the molecular complexity increases.

3. Decomposition Rates of Excited Reaction Complexes. Temperature Effects. We have measured the effect of temperature upon the rate constants, k_b, for the back-dissociations of the excited complexes involved in the reactions investigated. We find that the temperature coefficients of the rate constants vary with temperature; that is, the reaction rates do not have a simple functional dependence upon temperature. Representing this behavior in a convenient but meaningful way constitutes something of a problem. In the past we have represented[2,3] temperature coefficients by plotting ln k vs. ln T, and for lack of a better procedure we continue this practice here in Figure 4. As a measure of the temperature dependencies for the rate constants, we have measured the slopes at 375°K of the experimental plots in Figure 4, and the results expressed as $k_b = AT^n$ are given in Table II. A more detailed consideration of these temperature dependences will be given later in this paper.

Third-order rate constants for our reactions are meaningful only at the low-pressure limit, and may be calculated from our data as

$$k_3 = k_c k_s / k_b \quad (7)$$

To facilitate comparisons of our results with rate constants for other ion–molecule association reactions, which are generally published as k_3, we calculated k_3 for our reactions at 250 and 350°K using eq 7. The values, which are rather large negative temperature dependences. At 375°K these are $T^{-3.2}$ for reaction I, $T^{-3.6}$ for II, and $T^{-7.2}$ for III; the last is the largest negative temperature dependence observed for any ion–molecule reaction to date. The energy-third-order association rate constants therefore exhibit large negative temperature dependences. At 375°K these are $T^{-3.2}$ for reaction I, $T^{-3.6}$ for II, and $T^{-7.2}$ for III; the last is the largest negative temperature dependence observed for any ion–molecule reaction to date. The energy-transfer RRKM theory predicts increasing negative temperature dependence with increasing molecular complexity. This is borne out in comparing reactions I, II, and III.

4. Observations of the Kinetics of the Clustering Reactions of $C_2H_5(CH_3)_2NH^+$ and $(C_3H_7)_2NH^+$. In order to examine the dependence of reaction kinetics on further increase in molecular complexity, we attempted to conduct kinetics studies on the clustering reactions of $C_2H_5(CH_3)NH^+$ and $(C_3H_7)_2NH^+$. These reactions, however, appear to proceed with a mechanism different from the association reactions involving the smaller reactants. A typical pressure study is shown in Figure 5. The dependence of k_f on (M) does not follow the predictions of eq 6, and, furthermore, k_f levels off to a second-order limit which is different from the Langevin or ADO collision rate: e.g., for the case shown in Figure 4, it is about 0.25×10^{-9}, which is five times less than the ADO value of 1.26×10^{-9} cm³/(mol sec). Unlike the capture collision rate, this second-order limiting rate exhibits large negative temperature dependence. We cannot readily explain this behavior; we wish to note, though, that the size of the reactant molecules in these reactions approaches the critical Langevin collision

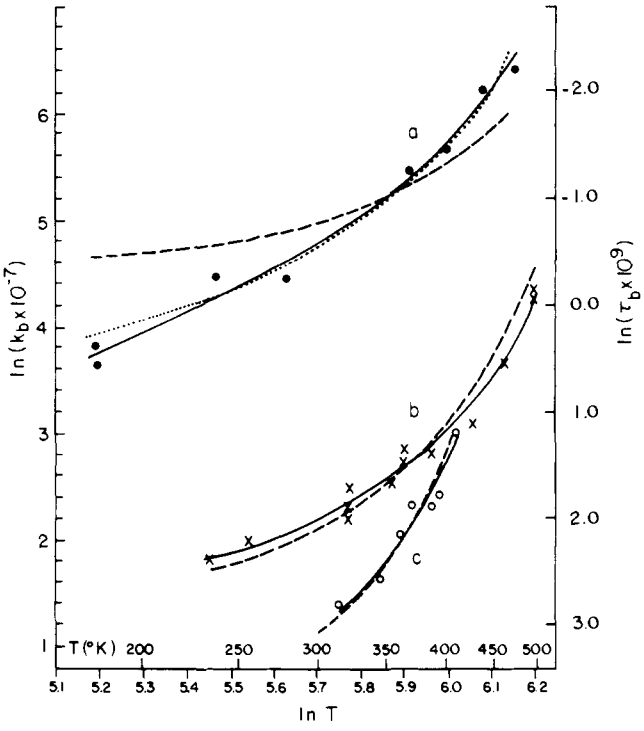

Figure 4. The temperature dependences of the dissociation rate constants k_b (in units of 10^7 sec^{-1}) and of the dissociation half-lives τ_b (in units of 10^{-9} sec) of the excited complexes: (a) $(NH_4^+ \cdot NH_3)^*$; (b) $(CH_3NH_3^+ \cdot CH_3NH_2)^*$; (c) $((CH_3)_2NH_2^+ \cdot (CH_3)_2NH)^*$. For ease of reference, the absolute temperature (°K) is also indicated. The broken lines give the theoretical temperature dependences predicted by eq 8 (vide infra), with $s = 3N - 6$ and $\bar{\nu} = 850$ cm^{-1}; for the dotted line in plot a $\bar{\nu} = 650$ cm^{-1} was used. For the sake of clarity the theoretical lines were translated such that they coincide with the experimental plots at 350°K, i.e., these are plots of $\ln [k_b^T(\text{calcd})(k_b^{350}(\text{exptl})/k_b^{350}(\text{calcd})]$ vs. $\ln T$, where the values of k_b^{350}(calcd) are 4.4×10^6, 5.3×10^5, and 3.7×10^4 for the broken lines in plots a, b, and c, correspondingly, and 3.2×10^6 for the dotted line in plot a.

parameter. The kinematics of ion-molecule reactions in which the size of the reactants is too large to permit the formation of orbiting complexes in the traditional sense presents an interesting problem.

Discussion

The kinetics of ion-molecule association reactions have been discussed up to the present time mostly in the context of the energy-transfer mechanism. The RRK model of the decomposition of a system of coupled oscillators considering s classical harmonics oscillators was used[3,11-13] to interpret the temperature dependence of k_b for the decomposition of ion-molecule association complexes. However, it is known[14,15] that the classical approximation can yield results which are significantly different from the predictions of the more accurate quantum oscillator model. We therefore, have carried out computations using the RRKM model with quantum oscillators, and we compare the results of such calculations to our experimental values of k_b. The details of the computations will be presented elsewhere.[15]

In the case of ion-molecule association reactions, the association complex derives energy from two sources: (1) the thermal energy of the reactants, and (2) the chemical energy of the exothermic association reaction. Thus the complexes are formed only with energies larger than $|\Delta H|$ for the reaction. We use the principle of microscopic reversibility and postulate the establishment of steady state populations in the manifold of possible energy states of the complex. The result of this treatment is that the relative concentrations of the complexes in the states with $E \geq |\Delta H|$ are

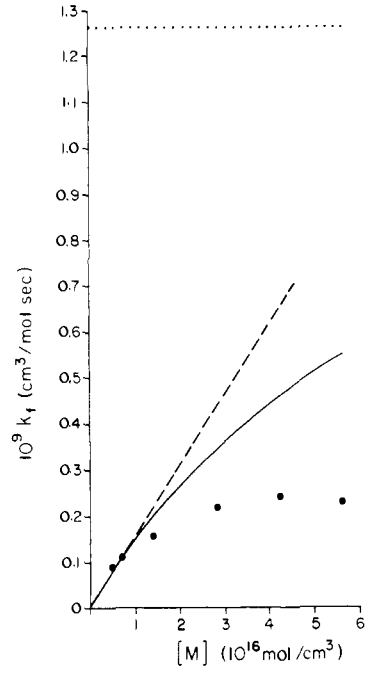

Figure 5. The dependence of the second-order rate constant k_f on third-body (i-C_4H_{10}) density for reaction $C_2H_5(CH_3)_2NH^+ + C_2H_5(CH_3)_2N$ (M) $\rightarrow (C_2H_5(CH_3)_2N)_2H^+$ at 354°K. The meaning of the symbols is as in Figure 2. Note that the experimental points level off at $\approx 0.25 \times 10^{-9}$ cm^3/(mol sec), rather than following the prediction of eq 6. The leveling off is far below the ADO bimolecular collision rate, 1.26×10^{-9} cm^3/(mol sec).

equal to the relative concentrations in a complete thermal equilibrium at the same temperature. That is to say, the populations of energy levels with $E < |\Delta H|$ are zero, but for $E \geq |\Delta H|$ the relative populations are identical with those which would be found in a thermal distribution over all the levels. The weight of each state is given by $S_{(j+n)} \cdot e^{-(j+n)h\nu/kT}$. Here j is the number of quanta in B_2H^+* arising from the exothermicity of the association process; i.e., $j = |\Delta H/h\nu|$. n is the number of thermal quanta; $S_{(j+n)}$ is a statistical weight equal to the number of ways in which $j + n$ quanta can be distributed over s oscillators; and $e^{-(j+n)h\nu/kT}$ is the Boltzmann factor for the state containing $j + n$ quanta. In the RRKM treatment that we apply,[16] the decomposing ion is taken as a coupled set of s quantum harmonic oscillators each of frequency ν. In ions with internal energy $E = (j + n)h\nu$ the total of $j + n$ quanta can be distributed over the s oscillators in many ways, and the RRKM treatment relates the rate constant k_b to the fraction of the total number of distributions that contain at least j quanta in the critical oscillator. By a direct counting of states we obtain the result

$$k_b = \frac{\sum_{n=0}^{\infty} S_{(j+n)} e^{-(j+n)h\nu/kT} \times \sum_{m=j}^{j+n} \nu \frac{(j+n-m+s-2)!(j+n)!(s-1)!}{(j+n+s-1)!(j+n-m)!(s-2)!}}{\sum_{n=0}^{\infty} S_{(j+n)} e^{-(j+n)h\nu/kT}} \quad (8)$$

The second sum in the numerator of eq 8 ($\sum_{m=j}^{j+n} \nu \ldots$) is identical (except for notation) with the molecular decomposition rate constant of the RRKM model as given by Johnston.[16]

The results of the calculations are summarized and compared with experiments in Table III. We carried out computations for systems of coupled quantum oscillators with s equal to the number of internal degrees of freedom in

Table III. Calculated (RRKM) and Experimental Effects of Molecular Complexity and Temperature on the Decomposition Rates and Excited Reaction Complexes

No.	Complex	Internal degrees of freedom $S = 3N - 6$	k_b^{350} (calcd),[a] 10^7 sec^{-1}	$1/k_b$II[b] Calcd	$1/k_b$II[b] Exptl	k_bII/k_bIII[b] Calcd	k_bII/k_bIII[b] Exptl	Calcd temp dependence of k_b[c] between 350 and 400°K: $\tilde{\nu}$ = 1750 cm^{-1}	$\tilde{\nu}$ = 850 cm^{-1}	Exptl
I	$(NH_4^+ \cdot NH_3)^*$	21	100	17.8	18.3			$T^{0.13}$	$T^{2.3}$	$T^{3.2}$
II	$(CH_3NH_3^+ \cdot CH_3NH_2)^*$	39	5.6			6.1	2.0	$T^{0.35}$	$T^{4.3}$	$T^{3.6}$
III	$((CH_3)_2NH_2^+ \cdot CH_3NH_2)^*$	57	0.91					$T^{0.36}$	$T^{6.3}$	$T^{7.2}$

[a] All the calculated values presented here except where indicated otherwise were calculated from eq 8, with $\tilde{\nu}$ = 1750 cm^{-1}, $S = 3N - 6$ as shown in column 3. Values of j for these calculations were selected such that $j\bar{h}\nu$ = 22 kcal/mol, the average experimental value for these reactions. The summation over n was carried out not to ∞ but to values which contribute less than 2% to the overall decomposition rates. [b] At 350°K. [c] The calculated temperature dependence is smaller at lower temperatures. Such behavior was observed experimentally in Figure 4 and in other ion–molecule association reactions.[3] The calculated temperature dependence given in this table is obtained from the ratio ln $(k_b^{400}(\text{calcd})/k_b^{350}(\text{calcd})/\ln 400/350$.

B_2H^+ *. Separate computations were performed for average frequencies of $\bar{\nu}$ = 500, 650, 750, 850, 1000, 1500, 1750, and 2000 cm^{-1}. For the absolute values of k_b at 350°K the best agreement with the experiment was obtained with $\bar{\nu}$ = 1750 cm^{-1}. The results are presented in Table III and may be compared with experimental values in Table II. We see that the absolute values of k_b are approximated to within a factor of 2 to 6 and the decrease of k_b with increasing molecular complexity is also well reproduced, considering the crude nature of the degenerate oscillator model.

The temperature dependences of k_b(exptl) and k_b(calcd) are shown in Figure 4. We observe that the functional form of the dependence of k_b(exptl) on the temperature can be reproduced very well by eq 8 when $s = 3N - 6$ is taken for each species and average frequencies of $\bar{\nu}$ = 650 cm^{-1} for complex I and $\bar{\nu}$ = 850 cm^{-1} for II and III are used. The low average frequencies required to reproduce the experimental temperature dependences indicate the greater contribution of low frequency, easily excited modes to the temperature dependences of k_b. Such rather low frequency modes are probably associated with the weak $\gtrless NH^+ \ldots N \lessgtr$ bonds in these complexes. The use of different frequency oscillators to explain the absolute values and temperature coefficients of the rate constants can easily be rationalized by the concept that in a real system oscillators with different frequencies will be present. The experimental temperature coefficients will be mainly determined by the thermal energy in the lower frequency oscillators and the absolute values by the distribution of the energy over all the oscillators, the mean frequency of which will be relatively high.

In a previous publication[17] we proposed a simple application of transition state theory (TST) to the temperature dependence of termolecular ion–molecule association reactions. The temperature dependence was interpreted on the basis of the temperature dependences of the transitional and rotational partition functions of the reaction complex and of the reactants:

$$k_3 = AT \frac{(T_{\text{trans}})^{3/2}(T_{\text{rot}})^{3/2}}{\prod_i (T_{\text{trans}}{}^{3/2})_i (T_{\text{rot}}{}^{3/2})_i} T_{\text{int rot}}{}^{r/2} \quad (9)$$

Here A is a constant; the product in the denominator is over the i reactants, and the term $T_{\text{int rot}}{}^{r/2}$ arises from the partition functions of the total number (r) of internal rotations created ($r > 0$) or destroyed ($r < 0$) upon the formation of the complex. In deriving eq 9 it was assumed that no vibrational degrees of freedom of the activated complex or of the reactants were activated; that is, the vibrational partition functions were all taken to be unity. We found that eq 9 represented well the experimental temperature dependencies of the rate constants of the association reactions of small ions and molecules.

The predictions of this model may be compared with our results if we recall that the temperature dependence of k_3 is equal to $1/k_b$. Equation 9 predicts a linear relation between ln k_3 (and ln $1/k_b$) and ln T. The curvature that is observed in the experimental plots of Figure 4 cannot be easily explained on the basis of eq 9. Inclusion of temperature terms from the partition functions of excited low-frequency vibrational modes in the complex will cause a curvature in the plots of ln k_3 vs. ln T based on eq 9, but the curvature will be of opposite sign to that observed experimentally. Thus transition state theory in the degree of sophistication entailed in the derivation of eq 9 does not appear to be satisfactory for the reactions presently investigated. Transition state theory may be applied to the present reaction systems only if it is used in conjunction with the energy transfer mechanism. Collision rates for k_c and k_s can be obtained from TST, and these may be combined with values of k_b obtained from RRKM considerations to obtain values of k_3.

Conclusion

In conclusion, our results demonstrate the applicability of the energy transfer mechanism to ion–molecule association reactions. The rate constants of the dissociation of the excited association complexes are in the range $\approx 10^9$–10^7 sec^{-1}. The dissociation rate constants decrease with increasing molecular complexity and increase with increasing temperature. These trends can be quantitatively reproduced by the coupled degenerate quantum oscillator RRKM model using $s = 3N - 6$ and $\bar{\nu}$ = 1750 to calculate the absolute values, and $\tilde{\nu}$ = 650–850 cm^{-1} for the temperature coefficients of k_b.

Acknowledgement. This work was partially supported by a grant from the National Science Foundation.

References and Notes

(1) D. P. Beggs and F. H. Field, *J. Am. Chem. Soc.*, **93**, 1567 (1971).
(2) J. J. Solomon, M. Meot-Ner, and F. H. Field, *J. Am. Chem. Soc.*, **96**, 3727 (1974).
(3) M. Meot-Ner and F. H. Field, *J. Chem. Phys.*, **61**, 3742 (1974).
(4) R. Yamdagni and P. Kebarle, *J. Am. Chem. Soc.*, **95**, 3504 (1973).
(5) T. Su and M. T. Bowers, *Int. J. Mass Spectrom. Ion Phys.*, **12**, 347 (1973).
(6) L. Hellner and L. W. Sieck, *J. Res. Natl. Bur. Stand., Sect. A*, **75**, 487 (1971).
(7) E. Rabinowich, *Trans. Faraday Soc.*, **33**, 283 (1937).
(8) D. K. Bohme, D. B. Dunkin, F. C. Fehsenfeld, and E. E. Ferguson, *J. Chem. Phys.*, **49**, 5201 (1968); E. E. Ferguson, "Ion-Molecule Reactions", Vol. 2, J. L. Franklin, Ed., Plenum Press, New York, N.Y., 1972, p 371.
(9) R. S. Hemsworth, J. D. Payzant, H. J. Schiff, and D. K. Bohme, *Chem. Phys. Lett.*, **26**, 417 (1974).
(10) M. Meot-Ner and F. H. Field, *J. Am. Chem. Soc.*, **97**, 2014 (1975).
(11) Reference 8, p 369.
(12) R. Wolfgang, *Acc. Chem. Res.*, **3**, 48 (1970).

(13) A. Good, *Trans. Faraday Soc.*, **67**, 3495 (1971).
(14) P. J. Robinson and K. A. Holbrook, "Unimolecular Reactions", Wiley-Interscience, London, 1972, p 62.
(15) M. Meot-Ner, Ph.D. Thesis, Rockefeller University, 1975.
(16) H. S. Johnston, "Gas Phase Reaction Rate Theory", Ronald Press, New York, N.Y., p 281.
(17) M. Meot-Ner, J. J. Solomon, F. H. Field, and H. Gershinowitz, *J. Phys. Chem.*, **78**, 1773 (1974).
(18) S. Glasstone, K. J. Laidler, and H. Eyring, "The Theory of Rate Processes", McGraw-Hill, New York, N.Y., 1941, p 220 ff.

Quantitative Definition of Exciton Chirality and the Distant Effect in the Exciton Chirality Method

Nobuyuki Harada,[1] Sow-mei Lai Chen, and Koji Nakanishi*

Contribution from the Department of Chemistry, Columbia University, New York, New York 10027. *Received January 29, 1975*

Abstract: The circular dichroism spectra (CD) of a series of steroidal glycol bis(*p*-dimethylaminobenzoates) have been measured and quantitatively calculated in order to clarify the distant effect in the exciton chirality method. An excellent agreement has been found between the experimental and theoretical curves. Theoretical calculations have shown that the intensity of the split Cotton effect is maximal at a dihedral angle of ca. 70°, and is inversely proportional to r^2 (where r is interchromophoric distance). This coupled Cotton effect is still observable for remote dibenzoates such as the 1,8-glycol dibenzoate (**10**) and hence should be useful for configurational studies of a variety of natural products. Taylor expansion of eq 9 representing the split CD Cotton effect gives $\mathbf{R}_{ij}\cdot(\boldsymbol{\mu}_{i0a} \times \boldsymbol{\mu}_{j0a})V_{ij}$ as a quantitative definition of exciton chirality for two interacting identical chromophores. The imbalance between the first and second apparent Cotton effects was found to originate from the asymmetrical pattern of the corresponding electronic absorption band.

There are two nonempirical methods for determining absolute configurations; one is the Bijvoet method of X-ray crystallography which is universally employed for various compounds, and the other is the optical method based on Davydov-split CD Cotton effects, which is applicable to compounds having more than two chromophores. The latter method has been studied extensively in the fields of biopolymers,[2] inorganic complexes,[3] physical chemistry,[4,5] as well as in organic chemistry.[6,7] Because of its nonempirical nature the method is more reliable than other empirical rules put forward for various organic chromophores.

We have proposed the exciton chirality method based on the dipole-dipole coupling mechanism and have determined the absolute configurations of various natural products.[7,8] A more quantitative treatment of coupled Cotton effects observed in steroidal glycol bis(*p*-dimethylaminobenzoate) systems[7,9] is given below together with experimental data for the purpose of clarifying the distant effect in practical applications of the exciton chirality method. Provided the angle between the electric transitions of two interacting chromophores does not change, the amplitudes of split CD curves are inversely proportional to the square of interchromophoric distances. On the other hand, in vicinal dibenzoates a maximum amplitude is expected at an interchromophoric angle of ca. 70°. A quantitative definition of exciton chirality is also described in this paper.

Theoretical Calculations

According to the molecular exciton theory,[10] when N identical chromophores possessing strong $\pi \rightarrow \pi^*$ transitions ($0 \rightarrow a$) interact with each other, the excitation wave number σ_k to the kth excited level of the whole system is represented by eq 1, where σ_0 is the excitation wave number

$$\sigma_k - \sigma_0 = \sum_{i=1}^{N} \sum_{j \neq i}^{N} C_{ik} C_{jk}^* V_{ij} \quad (1)$$

of the isolated noninteracting chromophore, C_{ik} and C_{jk}^* are coefficients of the corresponding kth wave function, and V_{ij} is the transition dipole interaction energy between two chromophores i and j.

Similarly, the kth rotational strength R^k due to the exciton coupling mechanism is

$$R^k = \pi\sigma_0 \sum_{i=1}^{N} \sum_{j \neq i}^{N} C_{ik} C_{jk}^* \mathbf{R}_j \cdot (\boldsymbol{\mu}_{j0a} \times \boldsymbol{\mu}_{i0a}) \quad (2)$$

where $\mathbf{R}_j$ is the distance vector from the origin to chromophore j, and $\boldsymbol{\mu}_{i0a}$ and $\boldsymbol{\mu}_{j0a}$ are electric transition moment vectors of groups i and j. If we take the real wave function for the N-mer and combine the two terms of $\mathbf{R}_j\cdot(\boldsymbol{\mu}_{j0a} \times \boldsymbol{\mu}_{i0a})$ and $\mathbf{R}_i\cdot(\boldsymbol{\mu}_{i0a} \times \boldsymbol{\mu}_{j0a})$, the following origin-independent formula of rotational strength is obtained

$$\sigma_k - \sigma_0 = 2 \sum_{i=1}^{N} \sum_{j>i}^{N} C_{ik} C_{jk} V_{ij} \quad (3)$$

$$R^k = -\pi\sigma_0 \sum_{i=1}^{N} \sum_{j>i}^{N} C_{ik} C_{jk} \mathbf{R}_{ij} \cdot (\boldsymbol{\mu}_{i0a} \times \boldsymbol{\mu}_{j0a}) \quad (4)$$

where $\mathbf{R}_{ij}$ is the interchromophoric distance vector from i to j, and V_{ij} (expressed in cm^{-1} unit) is approximated as follows

$$V_{ij} = \mu_{i0a}\mu_{j0a} R_{ij}^{-3} (\mathbf{e}_i \cdot \mathbf{e}_j - 3(\mathbf{e}_i \cdot \mathbf{e}_{ij})(\mathbf{e}_j \cdot \mathbf{e}_{ij})) \quad (5)$$

where $\mathbf{e}_i$, $\mathbf{e}_j$, and $\mathbf{e}_{ij}$ are unit vectors of $\boldsymbol{\mu}_{i0a}$, $\boldsymbol{\mu}_{j0a}$, and $\mathbf{R}_{ij}$, respectively.

Next, if a Gaussian distribution is approximated for the component CD Cotton effects, the curve of the kth Cotton effect is formulated as

$$\Delta\epsilon(\sigma)^k = \Delta\epsilon_{max}{}^k \exp\{-((\sigma - \sigma_k)/\Delta\sigma)^2\} \quad (6)$$

where $\Delta\epsilon_{max}{}^k$ is the maximum value of the Cotton effect, and $\Delta\sigma$ is the standard deviation of the Gaussian distribution. On the other hand, the kth experimental rotational strength R^k is expressed by

$$R^k = 2.296 \times 10^{-39} \int_0^\infty \Delta\epsilon(\sigma)^k/\sigma \, d\sigma = (2.296 \times 10^{-39}/\sigma_k) \int_0^\infty \Delta\epsilon(\sigma)^k \, d\sigma \text{ (cgs unit)} \quad (7)$$